06

Effect of buffer coatings on the structural state and magnetic properties of (Cr−Mn)/Fe films

© V.O. Vas'kovskiy,[1,2] A.A. Feshchenko,[1] M.E. Moskalev,[1] V.N. Lepalovskij,[1] E.A. Kravtsov,[1,2] A.N. Gorkovenko[1]

[1] Ural Federal University after the first President of Russia B.N. Yeltsin, Yekaterinburg, Russia
[2] M.N. Mikheev Institute of Metal Physics, Ural Branch, Russian Academy of Sciences, Yekaterinburg, Russia
e-mail: a.a.feshchenko@urfu.ru

Received February 14, 2023
Revised March 11, 2023
Accepted March 15, 2023

The article presents the results of a systematic study of the crystalline structure, microstructure, and hysteresis properties of $(Cr_{80}Mn_{20})$/Fe bilayers, deposited on buffer coatings of various metals (Cr, Fe, W, Ta). It has been established that depending on the composition of the buffer coating and the thickness of the Cr−Mn layer, the latter develops body-centered cubic structure with either the (110) or (200) texture, or none. It is shown that the Cr−Mn layer is a source of increased coercivity in the adjacent Fe layer and when is in a certain structural state and has a relatively large thickness (100 nm) induces exchange bias in the Fe layer. The regularities obtained are interpreted in terms of the antiferromagnetic ordering of Cr−Mn and its relatively weak magnetic anisotropy

Keywords: antiferromagnetics, ferromagnetic, bilayers, thickness, composition, temperature, texture, coercivity, exchange bias.

DOI: 10.21883/TP.2023.05.56070.24-23

Introduction

Thin-film magnetic materials are an effective functional medium, which is specifically applied in sensors and devices for high-density recording of information [1,2]. Layered structures of antiferromagnet/ferromagnet are among such materials due to the effect of exchange displacement realized in them, which consists in shifting the hysteresis loop of the ferromagnetic layer along the axis of magnetic fields [3,4]. In these structures, antiferromagnets play an auxiliary role, ensuring the fixation of the magnetic moment in functional ferromagnetic layers. However, in recent years, due to the observation of such effects as anomalous and spin Hall effects in them, antiferromagnets have also been considered as independent media for spintronics [5,6].

High-temperature antiferromagnetism, which has an applied value, is usually observed in Mn alloys with other transition metals. Moreover, sufficiently high functional properties are realized in systems containing platinum group metals such as Ir−Mn and Pt−Mn [7]. The search for alternatives that include less expensive components, among other things, leads to the Cr−Mn system, which in a fairly wide range of compositions is characterized by antiferromagnetic ordering with a high Neel temperature (over 600 K) [8]. The task is to realize this potential in the film state, and as part of a multilayer structure in the presence of an exchange bond between its antiferromagnetic and ferromagnetic components. The research experience accumulated in this field shows that quite serious physical and technological problems may arise along this path. The difficulties in obtaining the desired crystal lattice and optimal crystal texture in polycrystalline ferro- and antiferromagnetic layers are the most significant among them [9,10]. The use of so-called buffer coatings is one of the ways to influence the structural state of functional layers. These are thin auxiliary layers that are inserted between the substrate and the main film. Due to the epitaxy effect, they can set the type of crystal structure, create a crystalline texture in polycrystalline films, change the average size of crystallites and, in general, influence the magnetism of films through these factors [11,12]. This work is devoted to the study of the role of buffer coatings in the formation of the properties of double-layer films of the type (Cr−Mn)/Fe

1. Methodological aspects

It is known that the Cr−Mn alloy in a wide range of compositions is a solid solution of components and is characterized by a body-centered cubic (BCC) crystal lattice [13]. With this in mind, we used Ta, W, Sg, Fe, having a similar type of crystal structure, but differing in the lattice parameter a (0.331, 0.316, 0.289, 0.287 nm, respectively) and the type of magnetism (paramagnet, paramagnet, antiferromagnet, ferromagnet, respectively) for the development

of buffer coatings. In addition, the Fe layer was used as an indicator of the magnetic state of the adjacent layer Cr−Mn. In the case of the presence of an antiferromagnetic ordering in the latter, the coercive force of such a Fe layer will increase due to the interlayer exchange interaction, and a shift of the hysteresis loop can also be observed [3]. Most of the results in this study were obtained for a fixed ratio of components in the main layer — $Cr_{80}Mn_{20}$ and two values of its thickness L — 20 and 100 nm. According to the literature data, the specified composition falls into the concentration range in which the antiferromagnetic ordering is realized at room temperature in the Cr−Mn alloy and can be considered as a test. The variation of L is carried out for the reasons that the effect of exchange displacement in antiferromagnet/ferromagnet structures, the implementation of which this study is ultimately focused on, is very sensitive to the state of the microstructure of the antiferromagnetic layer, in turn, depending on its thickness [8]. The choice of specific thickness values was made on the basis of a preliminary experiment and reflects the presence of two magnetic states with significantly different and fairly stable reproducible properties. Thus, most of the samples studied had a layered structure characterized by the formula glass/Ta(5)/B(5)/$Cr_{80}Mn_{20}$(L)/Fe(10)/Ta(5), where the thicknesses of the layers in are indicated in parentheses. nm; L — the thickness of the binary layer, which took the values 20 and 100 nm; B — the component of the buffer coating, which in one case was absent, and in the other three was taken from the series Sg, Fe, W. The binary layer in such samples is denoted as Cr−Mn below. Along with this, several films with a different composition of the binary layer $Cr_{100-x}Mn_x$ $(10 < x < 70)$ or not containing a layer Cr−Mn — glass/Ta(5)/Fe(10)/Ta(5).

All films were obtained by magnetron sputtering at the AJA ATC Orion-8 facility using pure metal targets in sputtering or co-sputtering modes during deposition of one-component or two-component ($Cr_{100-x}Mn_x$) layers, respectively. Corning cover glass was used as a substrate. The metallic precipitates were produced under conditions of high-frequency electric displacement on the substrate and in the presence of a homogeneous magnetic field with a strength of 250 Oe (technological field), which was oriented parallel to the substrate plane. The pressure of the residual gases in the chamber was $5 \cdot 10^{-5}$ Pa, and the pressure of the argon working gas — $3 \cdot 10^{-1}$ Pa. The ratio of components in the Cr−Mn layer was monitored using a Rigaku Nanohunter X-ray fluorescence spectrometer. Structural studies were performed on a PANalytical Empyrean diffractometer in the radiation of Co,K_α and an Ntegra Prima scanning force microscope. EvicoMagnetics Kerr magnetometer was used to study the hysteresis properties of films at room temperature. Temperature measurements of magnetic properties were performed using system Quantum Design PPMS DynaCool.

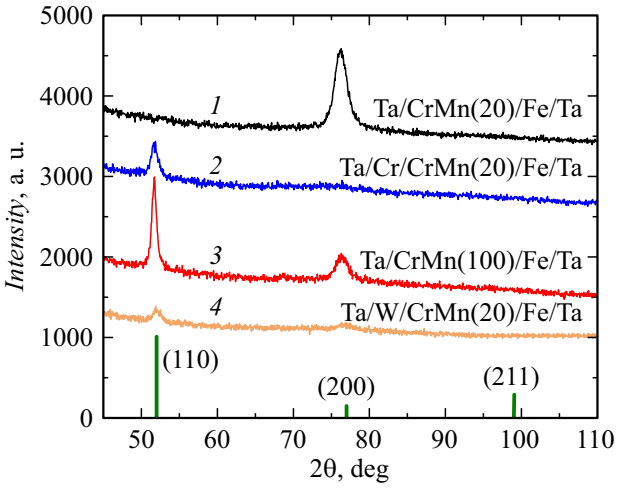

Figure 1. Diffractograms of film samples with layers Cr−Mn 20 nm thick (curves *1, 2, 4*) and 100 nm (*3*) on buffer coatings Ta (*1, 3*), Ta/Cr (*2*) and Ta/W (*4*). The vertical segments show the position of the calculated diffraction lines for polycrystalline Cr.

2. Experimental results and discussion

Systematic data were obtained during the completed study characterizing the crystal structure of multilayer films, the state of their surface and the hysteresis properties of the ferromagnetic component (Fe layer), which together are focused on determining the conditions for the implementation of antiferromagnetism in the Cr−Mn system in the film state and the role of the corresponding antiferromagnetic layer in the composition of a layered composite type (Cr−Mn)/Fe.

2.1. X-ray certification of the structural state of films

Fig. 1 shows the typical variants of X-ray diffractograms characteristic of the studied films by the example of samples containing buffer coatings Ta, Ta/Cr and Ta/W. In the same figure, vertical lines indicate the calculated position (taking into account the intensity ratio) of the diffraction lines for an isotropic polycrystal Cr. As can be seen, real diffraction reflexes can be identified as reflections from planes of the type (110) and (200) of the BCC lattice with very similar parameters. It can be assumed that this diffraction pattern is formed mainly by Cr−Mn layers (due to their greater thickness) and reflects the effect of crystal texturing, since it does not fully reproduce the calculated set of lines. Note also that the crystal lattice α-Fe has similar structural parameters. Its layers are present in all films and have a thickness of 10 nm, which is comparable to the thickness of Cr−Mn layers. Therefore, it is likely that Fe also makes a certain contribution to the diffraction pattern, while reproducing the texture of the underlying layer.

To clarify the conclusion about the presence of a crystalline texture, the technique of X-ray swing curves [14] was used. Figure 2 shows the corresponding curves measured

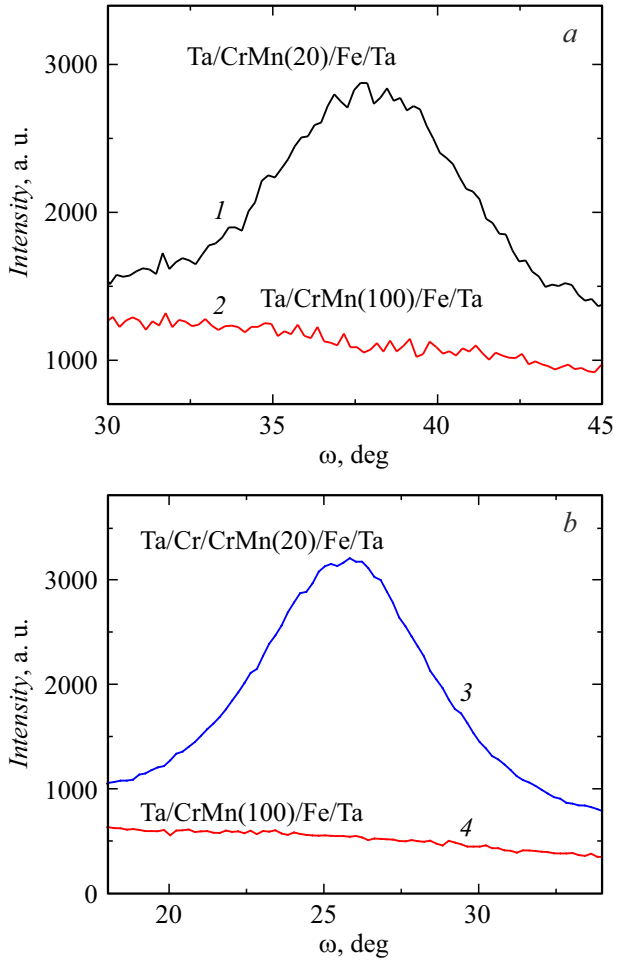

Figure 2. Swing curves measured on diffraction lines: *a* — (200); *b* — (110). Curves *1* and *3* correspond to diffractograms *1* and *2* (Fig. 1), curves *2* and *4* — diffractogram *3* (Fig. 1).

on different samples for the detected diffraction peaks. The presence of a pronounced maximum in the dependences of the X-ray intensity on the swing angle on the curves *1* and *3* is an unambiguous evidence of a crystal texture of the type (200) or (110). There are also non-textured states are also realized at the same time (curves *2, 4*). The presented X-ray data are illustrative and show that the studied films are prone to texture formation, and its implementation is influenced by both the buffer coating material and the thickness of the base layer Cr–Mn.

The summary results of the structural study are reflected in Table 1. According to them, it can be concluded that buffer coatings with B = Cr, Fe, whose crystal lattices are close in parameters to the lattice of the layer Cr–Mn, lead to the formation in this a layer of a crystalline texture of type (110), which is stable with respect to the variation of its thickness. An alternative option gives a buffer coverage of Ta. A different texture can be formed in such samples — (200). But it is less stable and degrades with increasing layer thickness Cr–Mn. Films coated with B = W demonstrate an intermediate situation in some way. A texture of the type (110) is formed in them, but only with a relatively large *L*. The most probable reason for such diversity in the structural state of the films is the difference in the ratio between the parameters of the buffer coating lattice and the Cr–Mn layer. If it is insignificant for Cr and Fe, then for W and, especially Ta, it is very large. Thus, the data obtained, on the one hand, can be considered as a method of controlled structure formation in thin films with a BCC lattice, and, on the other hand, it is necessary to take into account when analyzing the magnetic properties of the objects under study.

2.2. Certification of the microstructure of films using force microscopy

The magnetic properties of thin metal films, and, first of all, magnetic hysteresis, are very sensitive to the relief of surfaces [15,16]. In polycrystalline films, the inhomogeneities of the relief (roughness) can correlate both with the size of their own crystallites and reflect the state of the substrate surfaces or underlying layers of other metals. The latter circumstance was used by us to obtain indirect information about the microstructure of Cr–Mn layers using atomic force microscopy (AFM).

Figure 3 shows as an example AFM images of the surfaces of three samples, the diffractograms of which were discussed above. Formally, they reflect the relief of the surface of the Ta layer, which plays a protective role. However, due to the small thickness of the Ta, it can be assumed that it reproduces the relief of the layers lying below, i.e. Fe and Cr–Mn, which make up the bulk of the material in all films. Thus, the differences in relief should, first of all, correlate with the microstructure of these layered components, of which, in our opinion, the layer Cr–Mn plays a decisive role. It has a large thickness and serves as a structurally variable basis for Fe layers. Visually presented relief patterns have noticeable differences, but it is hardly advisable to discuss them at a qualitative level. It will be more informative to refer to a quantitative description of the surface relief in the form of a standard roughness parameter S_a.

The values of S_a are shown directly on the relief images and allow us to conclude the following. Firstly, the maximum amount of roughness in these samples, as a rule, does not exceed 0.3 nm, which indirectly indicates a fairly good surface quality of the substrates and gives reason to associate the features of the relief of the films with their microstructure. Secondly, against this background, there is a big difference in the values of S_a for films with different layered structures. In particular, the roughness increases more than twofold with an increase in the thickness of the *L* layer Cr–Mn from 20 to 100 nm (cf. Fig. 3, *a* and *c*). This is quite an expected effect, which most likely reflects the corresponding increase in the average size of the crystallites Cr–Mn. In addition, the composition of the buffer coating also affects the roughness. The Ta/Cr coating leads to a much larger value S_a than the Ta coating

Table 1. Characteristics of the crystal texture of films with different buffer coatings and layer thickness Cr−Mn

L, nm	Buffer coating			
	Ta	Ta/Cr	Ta/Fe	Ta/W
20	(200) texture	(110) texture	(110) texture	Texture is missing
100	Texture is missing	(110) texture	(110) texture	(110) texture

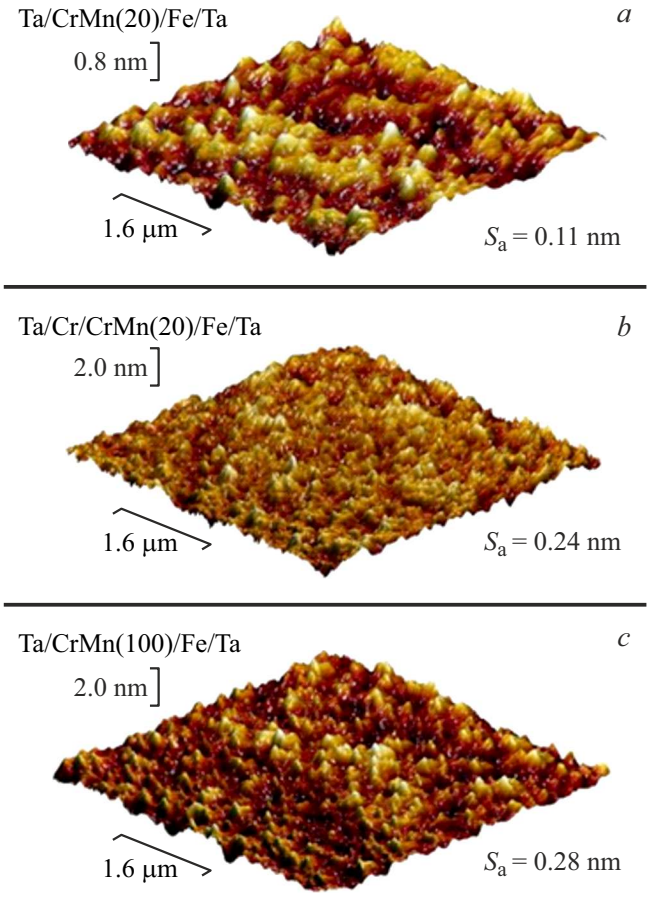

Figure 3. AFM images of the surfaces of film samples with layers of Cr−Mn with a thickness of 20 (a, b) and 100 nm (c) on buffer coverings Ta (a, c) and Ta/Cr (b).

(cf. Fig. 3, a and b). By analogy, linking this with the difference in the average size of Cr−Mn crystallites, we can talk about more favorable conditions for their growth on Cr compared to Ta. This conclusion correlates in a certain way with the result of the X-ray diffraction study (see above), according to which It contributes least to the texturing of Cr−Mn.

A summary of surface roughness data of samples of type A is provided in Table 2. Based on this table it is possible to additionally conclude that in the case of buffer coatings with B = Cr, Fe, the layer thickness Cr−Mn, at least within 20−100 nm does not significantly impact the roughness. These coatings, as shown above, initiate epitaxial

Table 2. Roughness values S_a of sample surfaces with different buffer coatings

L, nm	Buffer coating			
	Ta	Ta/Cr	Ta/Fe	Ta/W
20	$S_a = 0.11$ nm	$S_a = 0.24$ nm	$S_a = 0.19$ nm	$S_a = 0.23$ nm
100	$S_a = 0.28$ nm	$S_a = 0.19$ nm	$S_a = 0.21$ nm	$S_a = 0.39$ nm

Table 3. Hysteresis properties of samples with different layer thickness Cr−Mn on different buffer coatings: H_c — longitudinal coercive force; H_{ex} — exchange displacement field; ΔH_c — difference between values of coercive force determined from longitudinal and transverse hysteresis loops

L, nm	Buffer coating			
	Ta	Ta/Cr	Ta/Fe	Ta/W
20	$H_c = 43$ Oe $H_{ex} \sim 0$ $\Delta H_c \sim 0$	$H_c = 59$ Oe $H_{ex} \sim 0$ $\Delta H_c \sim 0$	$H_c = 70$ Oe $H_{ex} \sim 0$ $\Delta H_c \sim 0$	$H_c = 56$ Oe $H_{ex} \sim 0$ $\Delta H_c \sim 0$
100	$H_c = 65$ Oe $H_{ex} = 29$ Oe $\Delta H_c = 42$ Oe	$H_c = 80$ Oe $H_{ex} = 15$ Oe $\Delta H_c = 54$ Oe	$H_c = 94$ Oe $H_{ex} = 5$ Oe $\Delta H_c = 60$ Oe	$H_c = 99$ Oe $H_{ex} = 8$ Oe $\Delta H_c = 0$ Oe

buildup of Cr−Mn within the texture of type (110). A high texture, apparently, has a stabilizing effect on the planar size of the crystallites. There is a tendency of an increase of S_a with an increase of L in a sample with a buffer coating Ta/W, as well as in a sample with just a Ta coating. It is characteristic that this also occurs against the background of a thickness change in the crystal texture. Moreover, the presence of W in the accepted logic leads to the largest size of crystallites in a layer of Cr−Mn of large thickness.

2.3. Hysteresis properties of films on various buffer coatings

As noted above, Fe layer deposited on top of the Cr−Mn layer is considered by us in this study as a kind of indicator of the magnetic state of the latter. Therefore, the magnetic properties listed below relate specifically to this layer. In particular, Figure 4 shows magneto-optical hysteresis loops for three samples, the properties of which were discussed in the illustrative plan above, as well as for

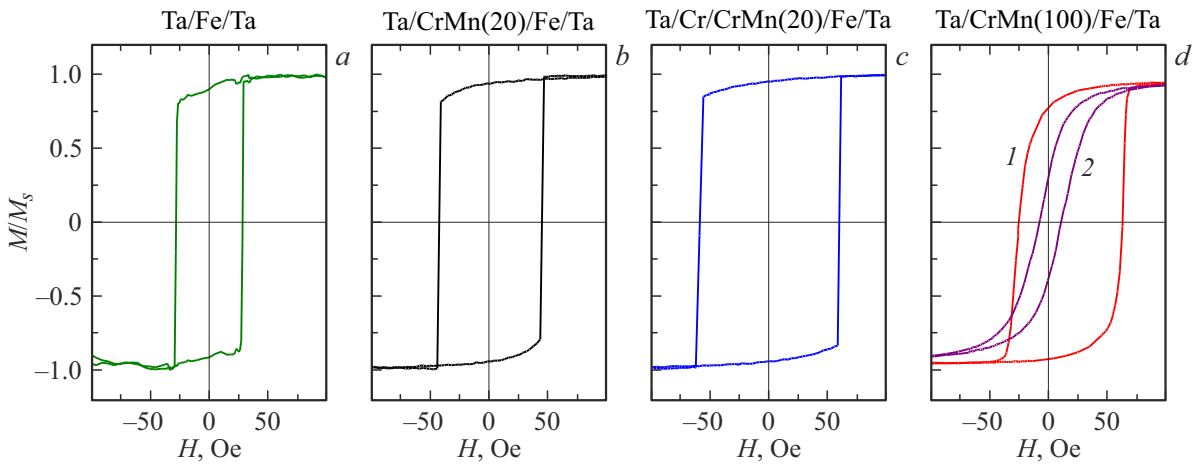

Figure 4. Magneto-optical hysteresis loops of the film glass/Ta/Fe(10)/Ta (*a*) and samples with layers Cr–Mn thickness 20 (*b*) and 100 nm (*d*) on buffer coverings Ta (*b, d*) and Ta/Cr (*c*). Digits *1* and *2* denote differing longitudinal and transverse hysteresis loops on the fragment (*d*), respectively. These loops are completely the same in three other cases (*a, c*).

comparing a film that does not contain a layer of Cr–Mn — glass/Ta/Fe(10)/Ta. The measurements were performed from the side of the film structure deposition in a magnetic field oriented in the plane of the films along (longitudinal hysteresis loops) and perpendicular (transverse hysteresis loops) the axes of the application of the technological field that was present when samples were received. The first and most important thing to note — is the increased hysteresis of Fe deposited on Cr–Mn. Coercive force H_c, determined from the longitudinal hysteresis loops (longitudinal coercive force) of all the samples studied (Table. 3), including those hysteresis loops that are shown in Fig. 4, *b, c, d*, exceeds the level of 50 Oe. At the same time, the typical value of H_c for a Fe film of the corresponding thickness does not exceed 30 Oe (Fig. 4, *a*).

These differences indicate a higher magnetic heterogeneity of the layers Fe by Cr–Mn, which may be a consequence of greater structural heterogeneity, for example, due to the developed surface relief. Analysis of the roughness of the glass/Ta/Fe(10)/Ta film gave a value of $S_a = 0.14$ nm, which is even higher than in the buffer-coated sample Ta (Table 2). It follows that the roughness and, probably, the state of the microstructure reflected by it, at this the level does not have a determining effect on the remagnetization. We believe that an abnormally high level of H_c is a sign of antiferromagnetic alignment in the layers of Cr–Mn. As is known, it can lead to increased hysteresis in exchange-bound structures of the ferromagnet/antiferromagnet type [3].

Table 3 shows that the value of H_c varies somewhat depending on the buffer coating material. However, this hardly needs to be given much importance due to the probabilistic nature of H_c itself. Another thing is more important — none of the films with $L = 20$ nm did not detect magnetic displacement (unidirectional magnetic anisotropy), which is an unambiguous sign of „ferro-antiferro“ exchange coupling. There were also no differences in the longitudinal and transverse hysteresis loops, which, in particular, is evidenced by the absence of a difference in the corresponding values of the coercive force ($\Delta H_c \sim 0$). Thus, these samples show almost complete isotropy of magnetic properties in the plane, although they were formed in a magnetic field, and for control they were also selectively subjected to subsequent thermomagnetic treatment — cooling in a magnetic field after heating to 250°C. It can be assumed that the reason for this is the low magnetic anisotropy of antiferromagnetic crystallites, which does not provide sufficient stability of the state and makes possible their magnetic switching together with the ferromagnetic layer.

The magnitude of the magnetic anisotropy energy of individual crystalline grains is determined by the anisotropy constant of the material and the volume of crystallites. In this connection, the regularities of the formation of hysteresis properties of films were investigated when the ratio of components in the system Cr–Mn, temperature and thickness of the specified layer were varied, assuming that the first two factors can affect the magnetic anisotropy constant, and the last — on the grain size. Fig. 5, *a* shows the dependence of the averaged longitudinal coercive force $\langle H_c \rangle$ on the concentration of Mn in layers $Cr_{100-x}Mn_x$. Averaging was performed for all types of buffer coatings in an effort to minimize the effect of random factors and to identify a general trend in the change of magnetic hysteresis. In addition, the magnitude of the coercive force of the sample without a layer Cr–Mn is included in the consideration. As can be seen, the dependence $\langle H_c \rangle(x)$ has a non-monotonic character. It shows a higher level of magnetic hysteresis just in the composition range in which the antiferromagnetic state [8] is realized on massive samples of the system $Cr_{100-x}Mn_x$ at room temperature. This is consistent with the provision that the increased coercive force of the Fe layer indicates the presence of antiferromagnetism in the adjacent layer Cr–Mn. However, magnetic displacement

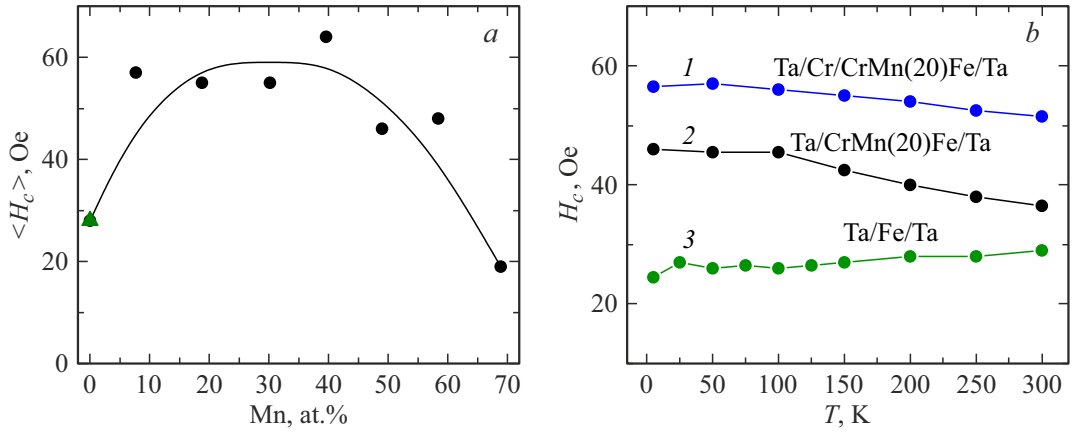

Figure 5. Concentration dependence of the averaged (for all types of buffer coatings) coercive force (a) for samples of type Ta/B/$Cr_{100-x}Mn_x$/Ta and temperature dependences of the longitudinal coercive force (b) for samples with $x = 20$ with buffer coatings Ta (curve *2*), Ta/Cr (curve *1*) and Ta/Fe/Ta films (curve *3*), the coercive force at room temperature, which is also indicated in the figure (a) by a triangle.

was not observed on any of the samples with $L = 20$ nm, which leads to the conclusion that the composition has a weak effect on the magnetic anisotropy of the system $Cr_{100-x}Mn_x$ under the condition of its antiferromagnetic ordering.

Fig. 5, *b* shows the temperature dependences of the longitudinal coercive force $H_c(T)$ for samples with buffer coatings Ta, Ta/Cr and for the Ta/Fe/Ta film. As can be seen, for them, along with a significant difference in the level of H_c, there is a difference in the nature of its change with temperature. For samples containing a layer Cr−Mn (curves *1, 2*), the coercive force clearly tend to increase with a decrease of the temperature, and in its absence it practically does not change within the error. Note also that temperature variation did not lead neither to any magnetic displacement ($H_{ex} \sim 0$), nor to the formation of anisotropy of properties ($\Delta H_c \sim 0$). All this, on the one hand, indirectly confirms the presence of antiferromagnetism in Cr−Mn and, apparently, reflects the temperature change in the magnitude of the magnetic anisotropy of this layer. On the other hand, it indicates that the probable increase in the magnetic anisotropy constant of the Cr−Mn layer at low temperatures is not sufficient for stabilization of the magnetic state of the corresponding crystallites and magnetic displacement.

The situation changed qualitatively with an increase in the layer thickness of Cr−Mn to 100 nm. Examples of corresponding longitudinal and transverse hysteresis loops of a sample on a buffer coating Ta are shown in Fig. 4, *d*. As you can see, the longitudinal loop is significantly displaced, and the transverse loop is much narrower than the longitudinal one. Summary data on the values of the longitudinal coercive force H_c, the exchange displacement field of the longitudinal loop H_{ex} and the difference between the longitudinal and transverse values of the coercive force ΔH_c in films with $L = 100$ nm, also provided in Table 3. An increase of coercive force with an increase of L is common pattern of all samples. This, as well as the presence of an exchange bias, is probably associated with an increase in the anisotropy energy of antiferromagnetic crystallites due to their enlargement. Following [17], it can be assumed that due to the dispersion in grain sizes, the larger grains ensure an exchange bias, while the smaller grains do not have sufficient resistance to switching and contribute to H_c.

However, the real picture is not so clear. Firstly, different buffer coatings lead to significantly different values of the exchange displacement field. If we look for a connection with the crystal structure in this, it is possible to state that the largest H_{ex} is obtained for a film on Ta in which there is no crystal texture. And in case of a strong texture of type (110), which is observed in films with B = Cr, Fe, the exchange displacement is much weaker. Secondly, there is no correlation between H_{ex} and ΔH_{ex}. Moreover, the magnetic anisotropy in the plane of the films, characterized by ΔH_c, is higher for textured samples on Cr and Fe. Taken together, these facts can be interpreted in the language of uncompensated magnetic moments on the surface of an antiferromagnet in contact with a ferromagnetic layer [18]. Probably, the crystal texture leads to a more ordered exchange bond between the ferromagnetic and antiferromagnetic layers, respectively, ΔH_c increases. But at the same time, the proportion of uncompensated magnetic moments on the interlayer interface decreases, which negatively affects H_{ex}.

Films on W with $L = 100$ nm demonstrate a slightly different variant of magnetic hysteresis, characterized by the largest H_c in a number of studied samples, the presence of weak magnetic displacement and the absence of magnetic anisotropy. Moreover, a texture of the type (110) is present, although not as pronounced as in films with B = Cr, Fe. This combination of properties is most likely a consequence of the specifics of crystal formation, due to which the grains Cr−Mn on W have a relatively large size (Table 2) and

are not textured in the plane. The first leads to a high H_c, and the second leads to planar magnetic isotropy.

Conclusion

In general, the presented results allow for making a conclusion that the crystal structure and antiferromagnetism characteristic of the Cr−Mn binary alloy are steadily reproduced in the thin-film state of this system, implemented using the magnetron sputtering method. The microstructure of such films can vary by changing their thickness and introducing buffer coatings with different parameters of the BCC lattice. A different combination of these factors leads to a crystalline texture of types (110) and (200) or to an untextured state. The same factors affect the hysteresis properties of the layered film structure (Cr−Mn)/Fe, and can provide a different level of coercive force, and with a certain combination — magnetic displacement of the ferromagnetic layer. However, the efficiency of Cr−Mn as a source of unidirectional anisotropy is relatively low, which is probably due to its low magnetic anisotropy.

Funding

This work was supported by grants from the RSF, project № 22-22-00814.

Conflict of interest

The authors declare that they have no conflict of interest.

References

[1] A.V. Ognev, A.S. Samardak. Vestnik Dalnevostochnogo otd. RAN, **4**, 70 (2006) (in Russian).
[2] I. Žutic, J. Fabian, S. Das Sarma. Rev. Modern Phys., **76**, 323 (2004). DOI: 10.1103/RevModPhys.76.323
[3] T. Blachowicz, A. Ehrmann. Coatings, **11**, 1 (2021). DOI: 10.3390/coatings11020122
[4] W.H. Meiklejohn, C.P. Bean. Phys. Rev., **105**, 904 (1957). DOI: 10.1103/PhysRev.105.904
[5] D. Xiong, Y. Jiang, K. Shi, A. Du, Y. Yao, Z. Guo, D. Zhu, K. Cao, S. Peng, W. Cai, D. Zhu, W. Zhao. Fundamental Research, **2**, 522 (2022). DOI: 10.1016/j.fmre.2022.03.016
[6] V. Baltz, A. Manchon, M. Tsoi, T. Moriyama, T. Ono, Y. Tserkovnyak. Rev. Modern Phys., **90**, 015005 (2018). DOI: 10.1103/RevModPhys.90.015005
[7] G.W. Anderson, Y. Huai, M. Pakala. J. Appl. Phys., **87**, 5726 (2000). DOI: 10.1063/1.372502
[8] Y. Hamaguchi, N. Kunitomi. J. Phys. Society Jpn, **19**, 1849 (1964). DOI: 10.1143/JPSJ.19.1849
[9] V.O. Vas'kovskiy, V.N. Lepalovskij, A.N. Gor'kovenko, N.A. Kulesh, P.A. Savin, A.V. Svalov, E.A. Stepanova, A.A. Yuvchenko, N.N. Shchegoleva. Tech. Phys., **60** (2), 116 (2015). DOI: 10.1134/S1063784215010260
[10] A.N. Gor'kovenko, V.N. Lepalovskij, V.O. Vas'kovskiy, P.A. Savin, N.N. Schegoleva. Solid State Phenomena, **215**, 278 (2014). DOI: 10.4028/www.scientific.net/SSP.215.278
[11] N.P. Alley, G. Vallejo-Fernandez, R. Kroeger, B. Lafferty, J. Agnew, Y. Lu, K. O'Grady. IEEE Transactions on Magnetics, **44**, 2820 (2008). DOI: 10.1109/TMAG.2008.2001317
[12] T. Stobiecki, J. Kanak, J. Wrona, G. Reiss, H. Brückl. J. Magn. Magn. Mater., **316**, e998 (2007). DOI: 10.1016/j.jmmm.2007.03.168
[13] M. Venkatraman, J.P. Neumann. Bull. Alloy Phase Diagrams, **7**, 457 (1986). DOI: 10.1007/BF02867810
[14] A.A. Jara, I. Barsukov, B. Youngblood, Y.-J. Chen, J. Read, H. Chen, P. Braganca, I.N. Krivotov. IEEE Magn. Lett., **7**, 1 (2016). DOI: 10.1109/LMAG.2016.2590464
[15] K.G. Balymov, N.A. Kulesh, A.S. Bolyachkin, A.P. Turygin, V.O. Vas'kovskiy, O.A. Adanakova, E.V. Kudyukov. Phys. Metals Metallography, **119**, 923 (2018). DOI: 10.1134/S0031918X18100022
[16] Y.P. Zhao, R.M. Gamache, G.C. Wang, T.M. Lu, G. Palasantzas, J.T.M. De Hosson. J. Appl. Phys., **89**, 1325 (2001). DOI: 10.1063/1.1331065
[17] K. O'Grady, L.E. Fernandez, G. Vallejo-Fernandez. J. Magn. Magn. Mater., **322**, 883 (2010). DOI: 10.1016/j.jmmm.2009.12.011
[18] C. Mitsumata, A. Sakuma, K. Fukamichi, M. Tsunoda. Mater. Transactions, **47**, 11 (2006). DOI: 10.2320/matertrans.47.11

Translated by A.Akhtyamov